Design of a 5-17 GHz Wideband GaAs Low Noise Amplifier with Capacitive Feedback

K. Sowjanya
Department of Electronics and Communication Engineering, Central University of Karnataka, Kalaburagi, India
22dpece01@cuk.ac.in (corresponding author)

Parameshа
Department of Electronics and Communication Engineering, Central University of Karnataka, Kalaburagi, India
parameshap@cuk.ac.in

P. Shanthi
Department of Electronics and Telecommunication Engineering, RV College of Engineering, Bengaluru, India
shanthip@rvce.edu.in

K. Sreelakshmi
Department of Electronics and Telecommunication Engineering, RV College of Engineering, Bengaluru, India
sreelakshmik@rvce.edu.in

Received: 9 March 2025 | Revised: 5 April 2025 | Accepted: 19 April 2025

 DOI: https://doi.org/10.48084/etasr.10879

ABSTRACT

This paper presents a two-stage broadband Low Noise Amplifier (LNA) that uses a matching network and source degeneration technique, combined with Capacitive Feedback (CFB). The novelty of the design is the integration of CFB and source degeneration, in order to achieve a flat, wideband gain while maintaining a low Noise Figure (NF). The proposed LNA has its foundation in GaAs pHEMT technology and is simulated using the Keysight ADS software. The simulation results demonstrate that the LNA delivers a consistent gain of 23 dB and NF below 1.016 dB, while maintaining excellent input and output reflection coefficients of <-8 dB, across the operating range of 5 - 17 GHz.

Keywords–LNA; capacitive feedback; pHEMT; Noise Figure (NF); two-stage

I. INTRODUCTION

LNAs are essential parts of many communication systems. Their main purpose is to increase the strength of marginal signals while reducing the level of extra noise produced. In particular, the Ultra Wide-Band (UWB) LNAs are used for satellite and radar applications. The study of radar and Satellite Communication (SATCOM) systems is important because of the growing need for high-speed data connectivity. As stated in [1, 2] the Ku-band has been set aside for SATCOM because its uplink frequencies are between 13.75 and 15.5 GHz and its downlink frequencies are between 10.6 and 12.80 GHz. The C and X bands are assigned for radar systems, with frequency ranges of 4 to 8 GHz for the C–band and 8 to 12 GHz for the X-band. C-Band radars are widely used in meteorological systems due to their ability to detect precipitation and other atmospheric phenomena. They provide moderate resolution and perform well in varying weather conditions, including moderate rain. X-Band radars offer high resolution and are commonly used in high-precision applications, such as target tracking, military surveillance, and radar imaging. Studies have shown that in SATCOM, the receiver may get saturated due to transmitter leakage signals. Furthermore, in order to achieve optimal overall performance, it is crucial to achieve less power consumption, high 1-dB compression point (IP1dB), and better noise and gain performance [3, 4]. Authors in [5] presented a three stage Common-Source (CS) LNA designed at 38 GHz for satellite communication, with a gain of 27 dB.

GaAs pHEMTs have several important advantages over other semiconductor materials, especially in terms of the performance of LNAs. Therefore, they are frequently used in

LNA engineering, particularly for high-frequency applications, such as satellite communications, radar, and other RF systems. In [6], it was demonstrated that a three-stage GaAs LNA designed with the frequency-dependent feedback loop, can improve gain flatness and bandwidth. The 0.1-µm GaAs pHEMT device was used in [7] to create a tapered distributed low-noise amplifier. A low broadband average NF can be attained by optimizing the transistor tapering and also the gate and drain transmission lines. The GaAs LNA with a two-stage topology described in [8], has its linearity enhanced by a diode-based adaptive bias circuit. In [9], a transistor width is tapered in the intended multistage circuit to improve linearity. Moreover, there is a feedback circuit to recompense for the roll-off between the transistor gain and the frequency. However, the strategies mentioned above, cannot achieve low NF and high small-signal gain simultaneously.

Numerous methods have been used to increase the bandwidth, including an LNA that utilized a pHEMT based GaAs device, to operate over the range of 6.5 - 16.5 GHz [10]. The LNA achieved a high gain by using the cascode structure. It also deployed source degeneration to stabilize the circuit. According to the results, the NF was between 1-2 dB, and the overall gain was 12.5 dB. However, the operational frequency was insufficiently high, the flatness was suboptimal, and the bandwidth was constrained. In [11], a 2-stage CS architecture was proposed to bring off a maximum gain of 43.3 dB and a minimum NF of 0.34 dB, despite the limited bandwidth of 0.4 GHz. To attain a further gain of 20-21 dB, authors in [12] created a balanced LNA that works for the range of 3.2- 3.8 GHz. Authors in [13] demonstrated that the bandwidth of 3.7–10.5 GHz was widened using the CS structure, despite the fact that the gain was less than 12 dB. Another study showed that the amplifier with a CS topology and an RC feedback network achieved 28 dB gain at the 4–16 GHz range, even though the NF was greater than 2 dB [14]. By combining the source degeneration technique, negative feedback, and CS structure, authors in [15] attained a gain of 29.1dB over the 12-18 GHz range. Authors in [16] described a three-stage cascade topology to create an LNA with 1–40 GHz bandwidth. Adding CS topology simultaneously, boosted its gain but it also increased power consumption and noise.

The current study presents a two-stage CS cascade LNA that uses GaAs pHEMT for radar and satellite applications. The combination of CFB with inductive source degeneration provides an optimal balance of gain, NF, bandwidth, and stability. The result is a highly effective technique for wideband GaAs pHEMT LNAs. CFB offers low-noise, power-efficiency, and high-gain operation when compared to resistive feedback. It is simpler to implement and has smaller losses compared to transformer feedback. Inductive degeneration enhances impedance matching and stability. These features make it superior to direct series or shunt feedback techniques. High-performance applications can benefit from the addition of a resistor at the output side of each stage to increase stability. Such applications are radars, satellite communications, and 5G systems. The NF of such a circuit is not raised because it is introduced at the output side. Since a new matching network technology was included in the design to boost bandwidth, the proposed LNA operates between 5 and 17 GHz. It has a lower NF of 1.016 dB and achieves a flat gain 23 dB in the band.

II. OVERVIEW OF THE CIRCUIT DESIGN

The objective of designing a two-stage cascaded LNA for high-frequency applications (satellite communications and radar) is to attain broadband performance, stability, linearity, maximum gain, and minimum NF over a large frequency range. The design incorporates several advanced techniques, such as inductive source degeneration, capacitive feedback, series resistors at the output side of each stage of the circuit, and low-pass filters designed as matching networks to ensure optimal performance. This design also improves impedance matching and signal amplification over a wide frequency range. The amplifier has two stages. Each one operates as a CS amplifier, as shown in Figure 1. The first stage amplifies the weak incoming signal. The second stage further amplifies it to the desired level, providing an overall high gain. In order to achieve higher gain, maintain a low NF, and ensure that the circuit remains stable over a wide frequency range, a common approach to use is cascading.

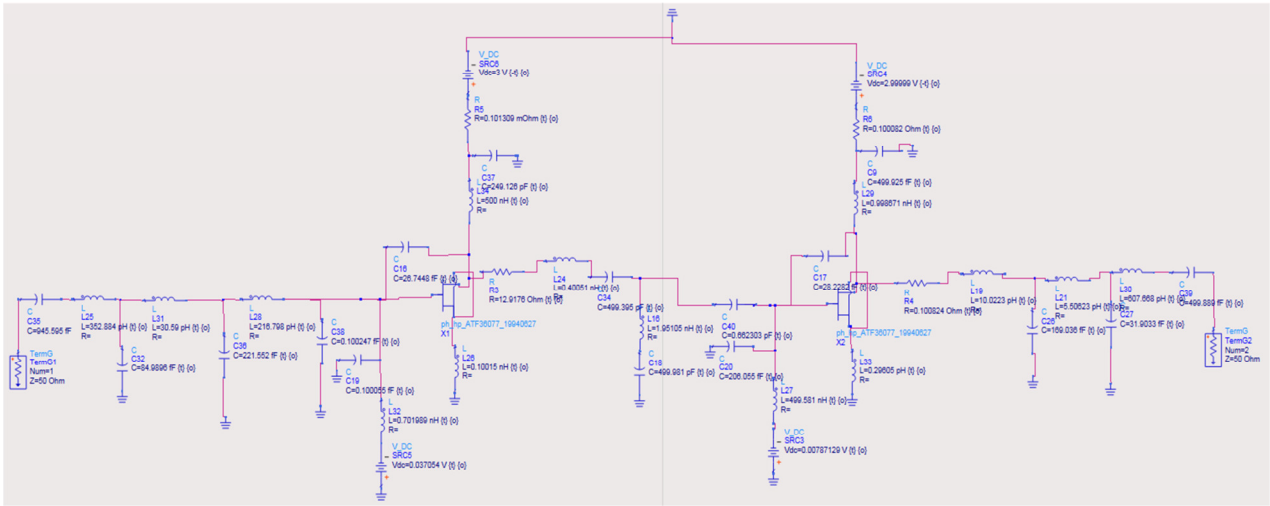

Fig. 1. Schematic diagram of the proposed two-stage LNA.

A. Inductive Source Degeneration

Inductive source degeneration is employed in each stage to improve the NF and linearity of the amplifier. The inductor is placed in series with the source terminal of the transistor, in order to reduce the NF by improving impedance matching at the source of the transistor. Moreover, its role is to linearize the transistor's characteristics, reduce non-linearities, and improve the signal fidelity. By decreasing the transistor's dependence on internal variations, the amplifier's gain is stabilized.

An inductor is utilized in the CS stage's source to produce inductive source degeneration. This inductor impacts the LNA's noise and gain performance. The MOS transistor's input impedance, has a resistive term due to the degenerated inductance in the CS stage's source. CS and cascade LNA circuits make extensive use of this approach [17 - 20].

B. Capacitive Feedback

CFB is applied at both stages to attain flat gain over a broad frequency range. The capacitor is connected between the drain and the gate of each transistor stage. It improves the bandwidth by compensating for any gain variation across the frequency range. It also stabilizes gain and minimizes distortion, thus ensuring that the signal is amplified without introducing significant harmonic distortions.

A resistor is placed at the output side of each stage to improve the impedance matching between the amplifier stages and the next stage. This resistor also serves for purposes, such as gain control, output impedance matching, and damping. Additionally, it may help dampen high-frequency oscillations or resonances that could arise in the output stage due to parasitic elements. Finally, the resistor plays an important role in stability; it stabilizes the circuit without increasing the noise in the signal.

C. Mathematical Modeling

The LNA consists of three blocks, i.e., input matching, transistor model, and output matching network.

Input matching network: The circuit consists of three inductors in series and capacitors in shunt. The Laplace transforms of inductors and capacitors are represented as:

$$L25 = sL1,\ L31 = sL2,\ L28 = sL3$$

$$C32 = \frac{1}{sC1},\ C36 = \frac{1}{sC2},\ C38 = \frac{1}{sC3}$$

The effective impedance works backward from the load.

Impedance at Node 3:

$$Z3 = \left(\frac{1}{Zc3} + \frac{1}{Zload}\right)^{-1} \quad (1)$$

Substituting $Zc3 = \frac{1}{sc3}$:

$$Z3 = \left(sc3 + \frac{1}{Zload}\right)^{-1} \quad (2)$$

Impedance at Node 2:

$$Z2 = \left(sc2 + \frac{1}{sL3+Z3}\right)^{-1} \quad (3)$$

Impedance at Node 1:

C1 is in parallel with L2 and Z2

$$Z1 = \left(sc1 + \frac{1}{sL2+Z2}\right)^{-1} \quad (4)$$

The total impedance seen at the input is:

$$Zin = sL1 + Z1 \quad (5)$$

The transfer function of the input matching network is given by:

$$H(s) = \frac{V_{out}}{V_{in}} = \frac{Z3}{Zin+Z3} \quad (6)$$

Expanding

$$H(s)_{IMN} = \frac{Z3}{sL1+Z1+Z3} \quad (7)$$

Similarly, for an output-matching network that has three inductors in series and two capacitors in parallel:

$$L19 = sL1,\ L21 = sL2,\ L30 = sL3$$

$$C26 = \frac{1}{sC1},\ C27 = \frac{1}{sC2}$$

The overall transfer function of the output matching network is given by:

$$H(s)_{OMN} = \frac{Z2}{sL1+Z1+Z2} \quad (8)$$

The inter-stage matching network is designed using a band-pass filter. The transfer function is given by:

$$H(s)_{BPF} = \frac{w_0^2}{s^2+\frac{w_0}{Q}s+w_0^2} \quad (9)$$

where $w_0 = \frac{1}{\sqrt{LC}}$, $Q = \frac{w_0 L}{R}$

Transistor model: The transfer function of the transistor model derived by using the equivalent circuit of the GaAs pHEMT.

Gate impedance is given by:

$$Z_g = R_g + sLg + \frac{1}{sCpg} \quad (10)$$

where R_g= Gate resistance, Lg = Gate inductance, Cpg = Pad gate capacitance.

Intrinsic transistor parameters:

Voltage controlled current source:

$$I_d = g_m V_{gs} e^{-jwT} \quad (11)$$

Impedance of gate capacitance:

$$Z_{gs} = \frac{1}{sC_{gs}} \quad (12)$$

Drain source impedance:

$$Z_{ds} = \left(R_{ds} || \frac{1}{sC_{ds}}\right) \quad (13)$$

Feedback impedance:

$$Z_{gd} = \left(\frac{1}{sC_{gd}} + R_{gd}\right) \quad (14)$$

The gate-source voltage is given by:

$$V_{gs} = V_g - V_s \quad (15)$$

The voltage at the drain is given by:

$$V_d = I_d Z_d = g_m V_{gs} e^{-jwT} Z_d \quad (16)$$

since $V_{out} = V_d$, $V_{in} = V_g = I_g Z_g$.

The transfer function of the transistor model is given by:

$$H(s)_{Tran} = \frac{V_{out}}{V_{in}} = \frac{g_m V_{gs} e^{-jwT} Z_d}{Z_g + Z_s + (Z_{gd} || Z_{gs})} \quad (17)$$

The overall transfer function of the circuit is given by:

$$H(s)_{Total} = H(s)_{IMN} . H(s)_{Tran} . H(s)_{BPF} . H(s)_{OMN} \quad (18)$$

$$H(s)_{LNA} = \left(\frac{Z3}{sL1+Z1+Z3}\right) . \left(\frac{g_m V_{gs} e^{-jwT} Z_d}{Z_g + Z_s + (Z_{gd} || Z_{gs})}\right) . \left(\frac{w_0^2}{s^2 + \frac{w_0}{Q} s + w_0^2}\right) . \left(\frac{Z2}{sL1+Z1+Z2}\right) \quad (19)$$

The total power gain in a two-stage cascaded LNA is calculated by multiplying the power gains of the individual stages. By denoting the power gain of the first stage as G_{P1} and the voltage gain of the second stage as G_{P2}, then the total gain G_{Total} is:

$$G_{Total} = G_{P1} . G_{P2}$$

Each stage power gain G_P can be calculated using the following formula, which combines CFB and inductive source degeneration:

$$G_P = \left| \frac{g_m R_L}{(1 + g_m j w L_s)(1 + j w C_f R_L)} \right|^2 \quad (20)$$

where g_m = transconductance of the transistor, R_L= load resistance at the output of the stage, L_s = inductance at source, C_f = capacitive feedback, w=2πf is the angular frequency, where f is the operating frequency.

The total NF for a two-stage cascaded LNA can be calculated using the Friis NF formula. The total NF depends on the NFs of the individual stages and the gain of the preceding stage. The formula is:

$$NF_{Total} = NF_1 + \frac{NF_2 - 1}{G_1} \quad (21)$$

where NF_1 = First stage NF, NF_2 = Second stage NF, G_1 = First stage gain.

The NF of each stage, considering CFB and inductive source degeneration, can be approximated using:

$$NF = 1 + \frac{R_n}{R_s} \left(\frac{|\Gamma_s - (\Gamma_{opt} + j w L_s + j w C_f R_L)|^2}{1 - |\Gamma_s|^2} \right) \quad (22)$$

where NF = Single stage NF, R_L = Load resistance, R_s = Source resistance, L_s = Source degeneration inductance, C_f = capacitive feedback, Γ_s = Source reflection coefficient, Γ_{opt} = Optimal reflection coefficient for minimum NF.

When designing amplifiers, it is important to verify that the amplifier operates within a stable region, in order to avoid issues, like undesired oscillations or instability, which can lead to distortion and performance degradation.

The stability factor of the K is defined as:

$$K = \frac{1 - |S_{11}|^2 - |S_{22}|^2 + |S_{11} S_{22} - S_{12} S_{21}|^2}{2 |S_{12} S_{21}|} \quad (23)$$

D. Low Pass Filter for Input and Output Matching and Band Pass for Inter-stage Matching

In order to ensure adequate impedance matching and improve the amplifier's frequency response throughout the 5–17 GHz range, multi section low-pass filters are made for both the input and output matching networks. Additionally, a multi section Band Pass Filter (BPF) is designed for inter stage matching network. The multi-section matching network is made up of cascaded inductive and capacitive elements and is used instead of a single-stage LC network, to gradually transform impedance over a wider range. These networks reduce reflection over a wider bandwidth, improve gain flatness by controlling frequency-dependent losses, and produce a more uniform frequency response, instead of a sharp resonant peak. Unlike simple LC networks, BPFs provide better gain shaping across a wide bandwidth by rejecting unwanted frequencies. This helps prevent oscillations and ensure stable operation. Series capacitors are used at the input as well as at the output sides of the amplifier. The input series capacitor blocks any DC component of the input signal and ensures that only the AC signal is passed into the amplifier.

III. RESULTS AND DISCUSSION

The proposed LNA's S parameters are depicted in Figures 2 and 3.

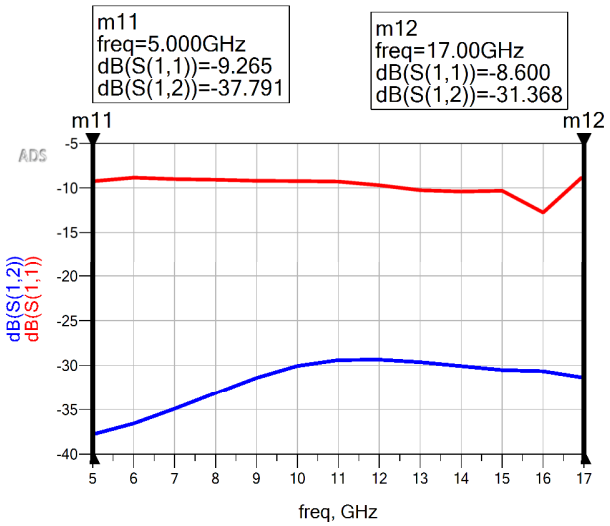

Fig. 2. Graph of S11 and S12 of the LNA.

S11 represents the signal reflection at port 1 when port 2 is matched (ended with a load). It measures the amount of the input signal at port 1 that the source reflects. S21 gives insight into the gain or loss of the network in the forward direction. S21 is commonly used to evaluate signal amplification or attenuation. S12 is used to assess how well the network

performs in the reverse direction. In some components, such as amplifiers, S12 is typically low (indicating little reverse transmission). S22 is the reflection at port 2 when port 1 is matched (terminated with a load). The amount of signal reflection back into the network at port 2 is displayed. It is analogous to S11, but for port 2. The stability factor K is calculated using the S-parameters of the amplifier, as illustrated in Figure 4, and it plays a key role in predicting and preventing self-oscillations.

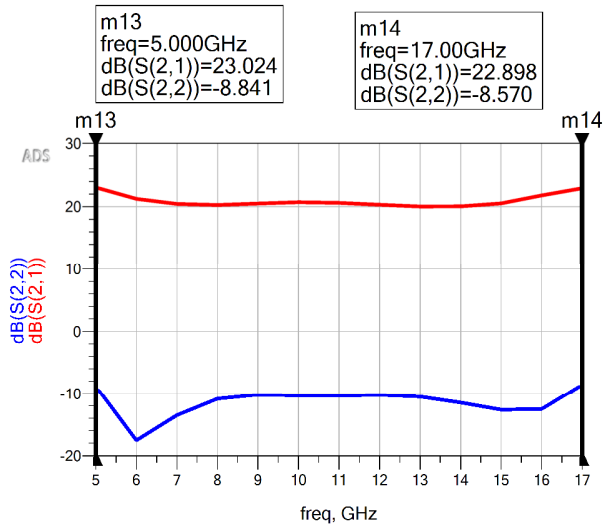

Fig. 3. Graph of S21 and S22 of the LNA.

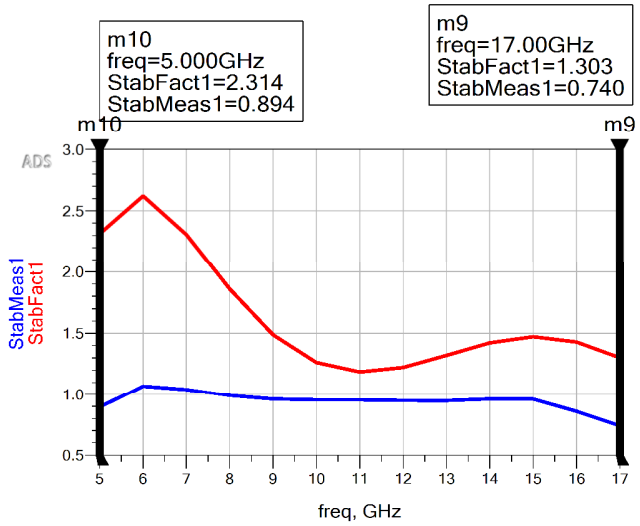

Fig. 4. Graph of stability factor and stability measurement of the LNA.

One important metric that measures the amount of noise that an amplifier adds to a signal, is the NF. It calculates how much the amplifier degrades the Signal-to-Noise Ratio (SNR), compared to the optimal situation/condition in which no noise is introduced. Figure 5 displays the proposed LNA's NF graph. The 1 dB compression point is the point where the amplifier's output is compressed by 1 dB compared to the expected linear output, with an input power of -5.5 dBm and an output power of 14.031 dBm, as portrayed in Figure 6.

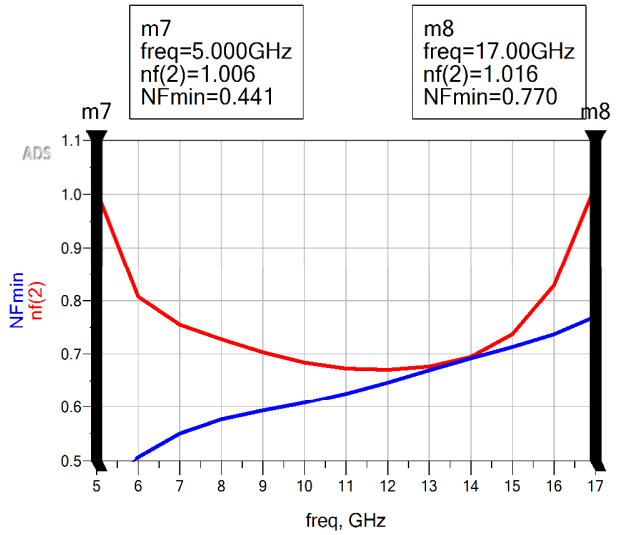

Fig. 5. NF graph of the LNA.

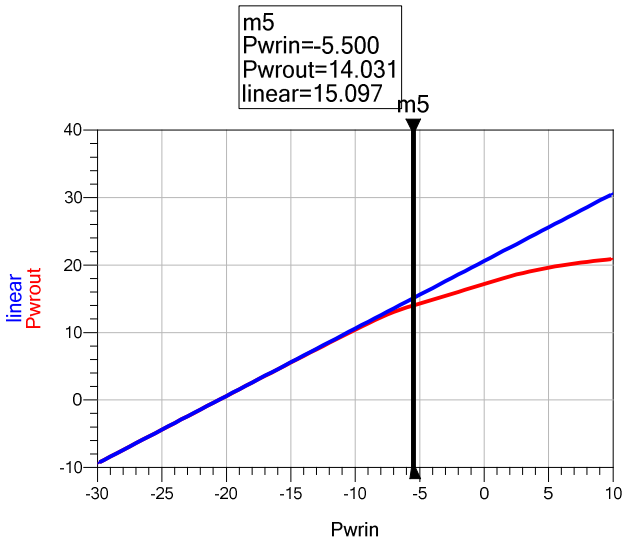

Fig. 6. 1 dB compression point of proposed LNA.

Table I presents the comparison of the proposed two-stage 5-17 GHz LNA with previous research. It is observed that the proposed work has better NFs and bandwidth compared to [21-24]. The technology and topology of the former studies are the same with the proposed work. The proposed LNA has better results compared to those of previous research, in terms of bandwidth, gain, NF, or reflection coefficients.

IV. CONCLUSION

Low Noise Amplifiers are indispensable in radar and satellite communication systems operating within the 5 to 17 GHz range. Their design focuses on minimizing noise addition while maximizing gain, which is essential for effective signal processing in these high-frequency environments. As technology advances, the development of more sophisticated LNAs will continue to enhance the performance of satellite communication and radar systems.

TABLE I. COMPARISON OF THE PROPOSED LNA PREVIOUS RESEARCH

Ref.	Technology	Topology	Freq. (GHz)	Gain (dB)	NF (dB)	S11/S22 (dB)
[21] 2018	GaAs pHEMT	3-stage CS	6~18	18	1.6~1.9	< -8, < -8
[22] 2023	GaAs pHEMT	2-stage CS&MRFB	1~12.5	23.6	1.51~2.4	< -8, < -10
[23] 2024	GaAs pHEMT	2- stage CS	13~14	23.2~25.5	1.6 ~2	< -11
[24] 2024	GaAs pHEMT	3-stage CS	6~14	26.8	1.21~1.53	< -15, < -15
This work	GaAs pHEMT	2- stage CS	5 ~ 17	23	0.7~1.016	< -8, < -8

The design and simulation of the 2-stage broadband Low Noise Amplifier (LNA) with Capacitive Feedback (CFB) and source degeneration, has demonstrated promising results for high-frequency applications. The proposed LNA satisfies the demanding specifications (minimal noise and satisfactory performance) in broadband applications, by attaining 23 dB flat gain over the range 5 to 17 GHz, with a Noise Figure (NF) below 1.016 dB. Additionally, the input and output reflection coefficients are less than -8 dB and demonstrate good impedance matching, assuring minimal signal loss and maximum power transfer.

REFERENCES

[1] J. Zhang, D. Zhao, and X. You, "Analysis and Design of a CMOS LNA With Transformer-Based Integrated Notch Filter for Ku-Band Satellite Communications," *IEEE Transactions on Microwave Theory and Techniques*, vol. 70, no. 1, pp. 790–800, Jan. 2022, https://doi.org/10.1109/TMTT.2021.3126858.

[2] M. Yang, D. Zhao, and X. You, "A Ku-Band CMOS Balanced Driver Amplifier With Transformer-Based Notch Filter for SATCOM Phased Arrays," *IEEE Transactions on Circuits and Systems II: Express Briefs*, vol. 70, no. 9, pp. 3318–3322, Sep. 2023, https://doi.org/10.1109/TCSII.2023.3268798.

[3] H. Gao *et al.*, "A 6.5–12-GHz Balanced Variable-Gain Low-Noise Amplifier With Frequency-Selective Gain Equalization Technique," *IEEE Transactions on Microwave Theory and Techniques*, vol. 69, no. 1, pp. 732–744, Jan. 2021, https://doi.org/10.1109/TMTT.2020.3038470.

[4] Y. S. Lai, Z. H. Fu, and K. Y. Lin, "Dual-input LNA for Switchable Daul-circular Polarization Satellite Receiver," in *2021 IEEE International Symposium on Radio-Frequency Integration Technology (RFIT)*, Dec. 2021, pp. 1–3, https://doi.org/10.1109/RFIT52905.2021.9565273.

[5] L. Balla and V. K. S. Gollakota, "A Low Noise Amplifier with 27 dB Gain and 1.78 dB Noise for Satellite Communications with 0.1 µm GaAs pHEMT Technology," *Engineering, Technology & Applied Science Research*, vol. 13, no. 5, pp. 11763–11767, Oct. 2023, https://doi.org/10.48084/etasr.6264.

[6] J. Hu, K. Ma, S. Mou, and F. Meng, "Analysis and Design of a 0.1–23 GHz LNA MMIC Using Frequency-Dependent Feedback," *IEEE Transactions on Circuits and Systems II: Express Briefs*, vol. 66, no. 9, pp. 1517–1521, Sep. 2019, https://doi.org/10.1109/TCSII.2019.2891262.

[7] G. Nikandish and A. Medi, "A 40-GHz Bandwidth Tapered Distributed LNA," *IEEE Transactions on Circuits and Systems II: Express Briefs*, vol. 65, no. 11, pp. 1614–1618, Aug. 2018, https://doi.org/10.1109/TCSII.2017.2758861.

[8] Z. Wang *et al.*, "A Linearity-Enhanced 18.7–36.5-GHz LNA With 1.5–2.1-dB NF for Radar Applications," *IEEE Microwave and Wireless Components Letters*, vol. 32, no. 8, pp. 972–975, Dec. 2022, https://doi.org/10.1109/LMWC.2022.3165124.

[9] G. Nikandish, A. Yousefi, and M. Kalantari, "A Broadband Multistage LNA With Bandwidth and Linearity Enhancement," *IEEE Microwave and Wireless Components Letters*, vol. 26, no. 10, pp. 834–836, Jul. 2016, https://doi.org/10.1109/LMWC.2016.2605446.

[10] L. He, J. Hu, and B. Gao, "A 6.5–16.5 GHz Low Noise Amplifier Based on GaAs pHEMT," in *2021 IEEE 3rd International Conference on Circuits and Systems (ICCS)*, Jul. 2021, pp. 144–149, https://doi.org/10.1109/ICCS52645.2021.9697166.

[11] T. Kulatunga, L. Belostotski, and J. W. Haslett, "400-to-800-MHz GaAs pHEMT-Based Wideband LNA for Radio-Astronomy Antenna-Array Feed," *IEEE Microwave and Wireless Components Letters*, vol. 28, no. 10, pp. 909–911, Jul. 2018, https://doi.org/10.1109/LMWC.2018.2864880.

[12] M. Uko, S. Ekpo, F. Elias, S. Alabi, "A 3.2-3.8 GHz Low-Noise Amplifier for 5G/6G Satellite-Cellular Convergence Applications," *e-Prime - Advances in Electrical Engineering, Electronics and Energy*, vol. 8, no. 100559, Jun. 2024, https://doi.org/10.1016/j.prime.2024.100559.

[13] Y. C. Hsiao, C. Meng, and M. C. Li, "Analysis and Design of Broadband LC-Ladder FET LNAs Using Noise Match Network," *IEEE Transactions on Microwave Theory and Techniques*, vol. 66, no. 2, pp. 987–1001, Oct. 2018, https://doi.org/10.1109/TMTT.2017.2760834.

[14] C. C. Huang, H. Y. Chang, and C. C. Chiong, "Stability Evaluation of a Broadband Multi-Stage Low Noise Amplifier using Nonlinear Analysis," in *2019 IEEE International Symposium on Radio-Frequency Integration Technology (RFIT)*, Nanjing, China, Dec. 2019, pp. 1–3, https://doi.org/10.1109/RFIT.2019.8929216.

[15] H. Kefeng and L. Jianping, "A Ku-band GaAs PHEMT low noise amplifier," *Journal of Microwaves,* vol. 33, no. 4, pp. 80-84, 2017.

[16] J. Hu and K. Ma, "A 1–40-GHz LNA MMIC Using Multiple Bandwidth Extension Techniques," *IEEE Microwave and Wireless Components Letters*, vol. 29, no. 5, pp. 336–338, Feb. 2019, https://doi.org/10.1109/LMWC.2019.2908883.

[17] H. Zhang, G. Chen, and X. Yang, "Fully Differential CMOS LNA and Down-Conversion Mixer for 3-5 GHz MB-OFDM UWB Receivers," in *2007 IEEE International Workshop on Radio-Frequency Integration Technology*, Sep. 2007, pp. 54–57, https://doi.org/10.1109/RFIT.2007.4443918.

[18] D. K. Shaeffer and T. H. Lee, "Corrections to A 1.5-V, 1.5-GHz CMOS Low Noise Amplifier," *IEEE Journal of Solid-State Circuits*, vol. 40, no. 6, pp. 1397–1398, Jun. 2005, https://doi.org/10.1109/JSSC.2005.848626.

[19] T. K. Nguyen, C. H. Kim, G. J. Ihm, M. S. Yang, and S. G. Lee, "CMOS low-noise amplifier design optimization techniques," *IEEE Transactions on Microwave Theory and Techniques*, vol. 52, no. 5, pp. 1433–1442, Feb. 2004, https://doi.org/10.1109/TMTT.2004.827014.

[20] T. H. Lee, *The Design of CMOS Radio-Frequency Integrated Circuits,* 2nd Edition, U.K., Cambridge Univ. Press, 1998.

[21] W. Xia, G. Dai, B. Li, C. Lyu, and L. Xu, "Design of a 6–18 GHz Low Noise Amplifier Using 0.25-um GaAs pHEMT D-Mode Technology," in *2018 International Conference on Microwave and Millimeter Wave Technology (ICMMT)*, Feb. 2018, pp. 1–3, https://doi.org/10.1109/ICMMT.2018.8563529.

[22] X. Yan, J. Zhang, H. Luo, S.-P. Gao, and Y. Guo, "A Compact 1.0–12.5-GHz LNA MMIC With 1.5-dB NF Based on Multiple Resistive Feedback in 0.15-µm GaAs pHEMT Technology," *IEEE Transactions on Circuits and Systems I: Regular Papers*, vol. 70, no. 4, pp. 1450–1462, Apr. 2023, https://doi.org/10.1109/TCSI.2023.3238361.

[23] A. Forte, P. E. Longhi, W. Ciccognani, S. Colangeli, A. Serino, and E. Limiti, "A Ku-Band MMIC Two-Stage GaAs-based Low Noise Amplifier for Radar Applications," in *2024 19th Conference on Ph.D Research in Microelectronics and Electronics (PRIME)*, Jun. 2024, pp. 1–4, https://doi.org/10.1109/PRIME61930.2024.10559714.

[24] D. He, N. Cui, J. Fan, and Z. Yu, "Design of Multiple Feedback-Based Low-Noise Amplifier With Improved Broadband Simultaneous Noise and Impedance Matching Technique," *IEEE Transactions on Circuits and Systems II: Express Briefs*, vol. 71, no. 2, pp. 582–586, Feb. 2024, https://doi.org/10.1109/TCSII.2023.3309380.